

General Disclaimer

One or more of the Following Statements may affect this Document

- This document has been reproduced from the best copy furnished by the organizational source. It is being released in the interest of making available as much information as possible.
- This document may contain data, which exceeds the sheet parameters. It was furnished in this condition by the organizational source and is the best copy available.
- This document may contain tone-on-tone or color graphs, charts and/or pictures, which have been reproduced in black and white.
- This document is paginated as submitted by the original source.
- Portions of this document are not fully legible due to the historical nature of some of the material. However, it is the best reproduction available from the original submission.

Auger and radiative deexcitation of the $1s2\ell 3\ell'$
configurations of lithium-like neon

(NASA-CR-149388) AUGER AND RADIATIVE
DEEXCITATION OF THE $1s2131$ PRIME
CONFIGURATIONS OF LITHIUM-LIKE NEON (Oregon
Univ.) 20 p HC A02/MF A01

CSCL 20L

N77-15873

Unclassified
G3/76 12367

Mau Hsiung Chen

Department of Physics, University of Oregon

Eugene, Oregon 97403

X-ray energies, Auger, and radiative decay rates and fluorescence yields have been computed in intermediate coupling for the various states of the $1s2s3s$, $1s2s3p$, $1s2p3p$, $1s2p3s$, and $1s2p3d$ configurations of ${}_{10}Ne^{7+}$, to supplement recent experimental work on these transitions.

*Work supported in part by the U.S. Army Research Office (Grant DAHC04-75-G-0021) and by the National Aeronautics and Space Administration (Grant NGR 38-003-036).

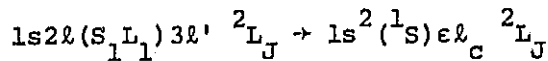
I. INTRODUCTION

The three-electron configurations $1s2\ell 3\ell'$ ($\ell = 0, 1$; $\ell' = 0, 1, 2$) of Ne have been observed in ion-atom collision^{1,2} and beam-foil excitation³ experiments. Knowledge of the Auger and fluorescence yields of these systems is needed to interpret the experimental results. In this paper, we report on a calculation of the pertinent multiplet Auger and x-ray transition rates obtained in intermediate coupling.^{4,5} The partial fluorescence yields were calculated for each state αJ that arises in a configuration n :

$$\omega_i(\alpha J, n) = \frac{\Gamma_i^R(\alpha J, n)}{\sum_i \Gamma_i^R(\alpha J, n) + \Gamma^A(\alpha J, n)}. \quad (1)$$

Here, Γ_i^R is the i th partial radiative width and Γ^A is the radiationless width of the decaying state. These partial fluorescence yields are useful to investigate the cascade feeding of other Li-like Ne configurations.⁶

II. AUGER TRANSITION RATES



The Auger transition rates for the pertinent multiplet states were derived in LS coupling. The Auger decay rate, in atomic units, is

$$A[(S_1 L_1) 2L_J] = |M(S_1 L_1 SL)|^2, \quad (2)$$

where the Auger matrix element $M(S_1 L_1 SL)$ is

$$\begin{aligned}
 M(S_1 L_1 SL) &= (-1)^{L+1} [(2\ell+1)(2\ell'+1)(2S_1+1)/2]^{1/2} \begin{pmatrix} \ell & \ell' & \ell_c \\ 0 & 0 & 0 \end{pmatrix} \\
 &\times \delta_{L\ell_c} \sum_{S_2=0,1} (2S_2+1) \begin{Bmatrix} 1/2 & 1/2 & S_1 \\ 1/2 & 1/2 & S_2 \end{Bmatrix} \left[(2\ell'+1)^{-1} \mathcal{R}_{\ell'} (1s\ell_c 2\ell 3\ell') \right. \\
 &\left. + (-1)^{S_2} (2\ell+1)^{-1} \mathcal{R}_{\ell} (1s\ell_c 2\ell 3\ell') \right]. \tag{3}
 \end{aligned}$$

We have

$$\mathcal{R}_k (1s\ell_c 2\ell 3\ell') = \int_0^\infty \int_0^\infty R_{1s}(r_1) R_{\ell\ell_c}(r_2) \frac{r_1^k}{r_2^{k+1}} R_{2\ell}(r_1) R_{3\ell'}(r_2) dr_1 dr_2, \tag{4}$$

where ϵ and ℓ_c are the energy and angular momentum of the continuum electron.

In the intermediate coupling scheme, the Auger rates are given by

$$A(\alpha J) = \left| \sum_{S_1 L_1} \sum_{LS} C(S_1 L_1 SLJ) M(S_1 L_1 SL) \right|^2, \tag{5}$$

where the $C(S_1 L_1 SLJ)$ are the mixing coefficients of the wave function for the state αJ .

III. THE MULTIPLET X-RAY TRANSITION RATES

The x-ray transition rates in LS coupling were calculated in dipole approximation, following the approach of Shore and Menzel.^{5,7} The x-ray rate, in atomic units, is given by

$$(2J+1) \mathcal{R}(\alpha SLJ, \alpha' S' L' J') = (4/3) k^3 S(\alpha SLJ, \alpha' S' L' J') \delta_{SS}, \tag{6}$$

where we have

$$S^{1/2}(\alpha SLJ, \alpha' S' L' J') = \langle \alpha' S' L' J' | | \Omega^{(1)} | | \alpha SLJ \rangle = \mathcal{R}_{\text{line}} \times \mathcal{R}_{\text{mult}} \times \mathcal{J}(\ell', \ell), \tag{7}$$

$$\alpha_{\text{line}} = [(2J+1)(2J'+1)]^{1/2} W(SJ'Ll;L'J), \quad (8)$$

and

$$J(\ell', \ell) = (-1)^{\ell' - \ell} \int \ell' \int p_{n' \ell'}(r) p_{n \ell}(r) r dr. \quad (9)$$

The wave number is

$$k = (E_i - E_f) / 27.21c, \quad (10)$$

where the energies E are in electron volts and c is the velocity of light.

The multiplet factors α_{mult} are listed in Table I.

IV. ELECTROSTATIC-INTERACTION MATRIX ELEMENTS FOR THREE-ELECTRON CONFIGURATIONS

The electrostatic-interaction matrix elements for three-electron configurations were derived using Racah algebra.⁷⁻⁹ The general expression is

$$\begin{aligned} v &= \langle \ell\ell' (L_1 S_1) \ell'' L S | \sum r_{ij}^{-1} | \ell\ell' (L_1' S_1') \ell'' L S \rangle \\ &= \sum_{L_2, S_2} F(\ell\ell'' L_2 S_2) [L_1, S_1, L_2, S_2]^{1/2} W(L_1 \ell'' \ell' L_2; L\ell) \\ &\quad \times W(S_1 \frac{1}{2} \frac{1}{2} S_2; S \frac{1}{2}) [L_1', S_1', L_2, S_2]^{1/2} W(L_1' \ell'' \ell' L_2; L\ell) \\ &\quad \times W(S_1' \frac{1}{2} \frac{1}{2} S_2; S \frac{1}{2}) + \sum_{L_3, S_3} F(\ell' \ell'' L_3 S_3) [L_1, S_1, L_3, S_3]^{1/2} \\ &\quad \times W(\ell\ell' L\ell''; L_1 L_3) W(\frac{1}{2} \frac{1}{2} S \frac{1}{2}; S_1 S_3) [L_1', S_1', L_3, S_3]^{1/2} \\ &\quad \times W(\ell\ell' L\ell''; L_1' L_3) W(\frac{1}{2} \frac{1}{2} S \frac{1}{2}; S_1' S_3) + F(\ell\ell' L_1 S_1) \delta_{L_1 L_1'} \delta_{S_1 S_1'}, \end{aligned} \quad (11)$$

where

$$F(\ell\ell''L_2S_2) = \sum_k [f_k(\ell\ell'')F^k(n\ell, n''\ell'') + g_k(\ell\ell'')G^k(n\ell, n''\ell'')] \quad (12)$$

$$f_k(\ell\ell'') = (-1)^{L_2} [\ell, \ell''] \begin{pmatrix} \ell'' & k & \ell'' \\ 0 & 0 & 0 \end{pmatrix} \begin{pmatrix} \ell & k & \ell \\ 0 & 0 & 0 \end{pmatrix} \begin{Bmatrix} \ell & \ell & k \\ \ell'' & \ell'' & L_2 \end{Bmatrix} \quad (13)$$

$$g_k(\ell\ell'') = (-1)^{S_2} [\ell, \ell''] \begin{pmatrix} \ell & k & \ell'' \\ 0 & 0 & 0 \end{pmatrix}^2 \begin{Bmatrix} \ell & \ell'' & k \\ \ell & \ell'' & L_2 \end{Bmatrix}. \quad (14)$$

and

$$[L_1, L_2, L_3, \dots] \equiv (2L_1+1)(2L_2+1)(2L_3+1)\dots$$

This notation is also used in Sec. V.

V. THE MATRIX ELEMENTS OF THE SPIN-ORBIT INTERACTION FOR THE $\ell^{n-2}\ell'\ell''$ CONFIGURATIONS

The matrix elements of the spin-orbit interaction for $\ell^{n-2}\ell'\ell''$ configurations were calculated following the procedure of Wybourne,¹⁰ through which the following expression can be derived:

$$(\ell^{n-2}\alpha_1 S_1 L_1 \ell' S_2 L_2 \ell'' S L' J M | H_{S-O} | \ell^{n-2}\alpha_1' S_1' L_1' \ell' S_2' L_2' \ell'' S' L' J M) \\ = (-1)^{S'+L+J} \begin{Bmatrix} S & S' & 1 \\ L' & L & J \end{Bmatrix} (A_{n\ell} \zeta_{n\ell} + A_{n'\ell} \zeta_{n'\ell'} + A_{n''\ell''} \zeta_{n''\ell''}), \quad (15)$$

where

$$A_{n\ell} = (-1)^{\delta_1} [S, S', L, L', S_2, S_2', L_2, L_2']^{1/2} \begin{Bmatrix} S & S' & 1 \\ S_2' & S_2 & \frac{1}{2} \end{Bmatrix} \begin{Bmatrix} L & L' & 1 \\ L_2' & S_2 & \ell'' \end{Bmatrix},$$

$$\times \begin{Bmatrix} S_2 & S_2' & 1 \\ S_1' & S_1 & \frac{1}{2} \end{Bmatrix} \begin{Bmatrix} L_2 & L_2' & 1 \\ L_1' & L_1 & \ell' \end{Bmatrix} [\ell(\ell+1)(2\ell+1)]^{1/2} (\ell^{n-2}\alpha_{SL} | | v^{(11)} | | \ell^{n-2}\alpha' S' L'), \quad (16)$$

$$\begin{aligned}
 A_{n' \ell'} &= (-1)^{\delta_2} \delta_{S_1 S_1', L_1 L_1'} [S, S', L, L', S_2, S_2', L_2, L_2']^{1/2} \\
 &\times (3\ell'(\ell'+1)(2\ell'+1)/2)^{1/2} \\
 &\times \left\{ \begin{array}{ccc} S & S' & 1 \\ S_2' & S_2 & \frac{1}{2} \end{array} \right\} \left\{ \begin{array}{ccc} L & L' & 1 \\ L_2' & L_2 & \ell'' \end{array} \right\} \left\{ \begin{array}{ccc} S_2 & S_2' & 1 \\ \frac{1}{2} & \frac{1}{2} & S_1 \end{array} \right\} \left\{ \begin{array}{ccc} L_2 & L_2' & 1 \\ \ell' & \ell' & L_1 \end{array} \right\}, \tag{17}
 \end{aligned}$$

$$\begin{aligned}
 A_{n'' \ell''} &= (-1)^{\delta_3} \delta_{S_2 S_2', L_2 L_2'} \delta_{L_1 L_1'} \delta_{S_1 S_1'} [S, S', L, L']^{1/2} \\
 &\times (3\ell''(\ell''+1)(2\ell''+1)/2)^{1/2} \left\{ \begin{array}{ccc} S & S' & 1 \\ \frac{1}{2} & \frac{1}{2} & S_2 \end{array} \right\} \left\{ \begin{array}{ccc} L & L' & 1 \\ \ell'' & \ell'' & L_2 \end{array} \right\} \tag{18}
 \end{aligned}$$

and

$$\delta_1 = S_2 + L_2 + S_2' + L_2' + S_1 + L_1 + S' + L' + \ell' + \ell'' + 1, \tag{19}$$

$$\delta_2 = 2S_2 + S_1 + L_1 + S' + L' + \ell' + \ell'' + 1, \tag{20}$$

$$\delta_3 = S_2 + L_2 + S + L + \ell'' + \frac{1}{2}. \tag{21}$$

Furthermore, we have

$$\begin{aligned}
 (\ell^{n-2} \alpha_{SL} | | v^{(11)} | | \ell^{n-2} \alpha' S' L') &= (n-2) \sqrt{\frac{3}{2} [S, L, S', L']}^{1/2} \\
 &\times \sum_{\overline{L}, \overline{S}} (\ell^{n-2} S_{\overline{L} \overline{S}} | | \ell^{n-3} \overline{S} \overline{L}) (\ell^{n-3} \overline{S} \overline{L} | | \ell^{n-2} S' L') \\
 &\times \left\{ \begin{array}{ccc} S & S' & 1 \\ \frac{1}{2} & \frac{1}{2} & \overline{S} \end{array} \right\} \left\{ \begin{array}{ccc} L & L' & 1 \\ \ell & \ell & \overline{L} \end{array} \right\} (-1)^{\overline{S} + \overline{L} + S + L + \ell + \frac{1}{2}}. \tag{22}
 \end{aligned}$$

VI. NUMERICAL CALCULATIONS

A. Atomic model

The single-particle wave functions used in the present calculations were generated through the Herman-Skillman¹¹ Hartree-Slater model with Kohn-Sham¹² exchange potential. The frozen-orbital approximation is used in the calculation of transition probabilities.

B. Auger and x-ray energies

Average Auger and x-ray energies were used for all multiplet transition-rate calculations. The Auger energies were taken from the work of Groeneveld et al.³ The x-ray energies were calculated using Froese's Hartree-Fock program¹³; they are listed in Table II.

C. Calculation of multiplet Auger and x-ray transition rates in intermediate coupling

Auger and x-ray transition rates were computed in LS coupling from expressions derived in Secs. II and III. Then the mixing due to spin-orbit interaction was included. The electrostatic-interaction matrix elements were evaluated from the formula derived in Sec. IV, and the spin-orbit interaction matrix elements were calculated from the expression obtained in Sec. V. The numerical values of the Slater integrals and spin-orbit parameters ζ_{nl} were calculated in the present atomic model. The mixing parameters $C(S_1 L_1 SLJ)$ in the intermediate coupling scheme were obtained by diagonalizing the energy matrix.

VII. RESULTS AND DISCUSSION

Auger and x-ray transition probabilities, as well as fluorescence yields ω_1 (LSJ), are listed in Tables III-VII for all initial states pertaining to the configurations $1s2s3s$, $1s2s3p$, $1s2p3p$, $1s2p3s$, and $1s2p3d$. All x-ray transitions with $\Delta n=1$ and $\Delta n=2$ are included. X-ray transitions with $\Delta n=0$ were neglected because their rates are of the order of 10^{-9} a.u., much smaller than the dominant branches in the decay of these states. Also neglected was the contribution due to the magnetic interaction to the Auger decay of the quartet states, estimated to be $\sim 10^{-9}$ a.u.¹⁴

It is seen from Table II that the x-ray energies fall into three distinct groups. One group comprises the range from 120 to 160 eV; these transitions have not been observed experimentally.^{1,2} A second group, with energies from 906 to 920 eV, will mix with x rays either from the KL^6 charge state or from the KL^7 charge state.^{1,2} The radiative transitions in the third group, from 1030 to 1050 eV, which originate from the $1s2s3p$ and $1s2p3p$ configurations, have been observed.^{1,2} The $1s2s3p$ and $1s2p3p$ configurations have the capability of feeding $1s2s^2$ and $1s2s2p$ configurations, respectively; this fact is consistent with the experimental observation that the $1s2s^2$ and $1s2s2p$ configurations are overpopulated.⁶

Most of the quartet states (cf. Tables III-VII) decay predominantly by L x-ray emission to the quartet states of the $1s2s2p$ and $1s2p^2$ configurations. As a result, multiplet states in the $1s2s2p$ and $1s2p^2$ configurations are populated nonstatistically, and furthermore, the x-ray intensity ratio $^4P/^2P$ of the KL^6 charge state is boosted. This increase in the KL^6 $^4P/^2P$ ratio will narrow the gap between the theoretically calculated⁵ and observed intensity ratios.

ACKNOWLEDGMENTS

The incentive for this study was provided by an inquiry from Professor K.-O. E. Groeneveld of the Johann Wolfgang Goethe-Universität, Frankfurt. The author is grateful to Professor B. Crasemann for his interest in this work and for helpful discussions.

REFERENCES

1. D. L. Matthews, B. M. Johnson, and C. F. Moore, Phys. Rev. A 10, 451 (1974); D. L. Matthews, B. M. Johnson, L. E. Smith, J. J. Mackey, and C. F. Moore, Phys. Lett. 48A, 93 (1974).
2. R. L. Kauffman, F. Hopkins, C. W. Woods, and P. Richard, Phys. Rev. Lett. 31, 621 (1973).
3. K. O. Groeneveld, R. Mann, G. Nolts, S. Schumann, R. Spohr and B. Fricke, Z. Physik A 274, 191 (1975) and K. O. Groeneveld, private communication.
4. M. H. Chen and B. Crasemann, Phys. Rev. A 10, 2232 (1974).
5. M. H. Chen and B. Crasemann, Phys. Rev. A 12, 959 (1975).
6. D. L. Matthews, R. J. Fortner, D. Schneider and C. F. Moore, Phys. Rev. A 14, 1561 (1976).
7. B. W. Shore and D. H. Menzel, Principles of Atomic Spectra (Wiley, New York, 1968); Astrophys. J. Suppl. Ser. 12, 187 (1965).
8. E. U. Condon and G. H. Shortley, The Theory of Atomic Spectra (Cambridge, U.P., Cambridge, England, 1953).
9. I. I. Sobel'man, Introduction to the Theory of Atomic Spectra (Pergamon Press, New York, 1972).
10. B. G. Wybourne, Spectroscopic Properties of Rare Earths (Wiley, New York, 1965).
11. F. Herman and S. Skillman, Atomic Structure Calculations (Prentice-Hall, Englewood Cliffs, N.J., 1963).
12. W. Kohn and L. J. Sham, Phys. Rev. 140, A1133 (1965).
13. C. Froese-Fischer, Comput. Phys. Commun. 4, 107 (1972).
14. K. T. Cheng, C. P. Lin, and W. R. Johnson, Phys. Lett. 48A, 437 (1974).

TABLE I. Multiplet factors.

Transition	α_{mult}	\mathcal{J}
$ss' (S_1 L) s'' SLJ \rightarrow ss' (S_1 L) pSL'J'$	1	$\mathcal{J}_{(p,s)}$
$ss' (S_1 L_1) pSLJ \rightarrow s^2 s' SL'J'$	$[(2s_1+1)/2]^{1/2}$	$\mathcal{J}_{(s,p)}$
$ss' (S_1 L_1) pSLJ \rightarrow ss' s^2 SL'J'$	$(-1)^{1-s_1} [(2s_1+1)/2]^{1/2}$	$\mathcal{J}_{(s,p)}$
$sp(S_1 L_1) p' SLJ \rightarrow s^2 pSL'J'$	$(-1)^L [(2s_1+1)(2L+1)/6]^{1/2}$	$\mathcal{J}_{(s,p)}$
$sp(S_1 L_1) p' SLJ \rightarrow s^2 p' SL'J'$	$[2(2L+1)/3]^{1/2} \delta_{S,0}$	$\mathcal{J}_{(s,p)}$
$sp(S_1 L_1) p' SLJ \rightarrow sp(S_1 L_1) s' SL'J'$	$(-1)^L [(2L+1)/3]^{1/2}$	$\mathcal{J}_{(s,p)}$
$sp(S_1 L_1) s' SLJ \rightarrow s^2 s' SL'J'$	$2^{1/2} \delta_{S,0}$	$\mathcal{J}_{(s,p)}$
$sp(S_1 L_1) s' SLJ \rightarrow sp^2 (S_1' L_1') SL'J'$	$(-1)^{S-1/2} (2/3)^{1/2} [s_1, s_1', s_1']^{1/2}$ $\times \left\{ \begin{array}{ccc} 1/2 & 1/2 & s_1 \\ s & 1/2 & s_1' \end{array} \right\}$	$\mathcal{J}_{(p,s)}$
$sp(S_1 L_1) dSLJ \rightarrow s^2 dSL'J'$	$[2(2L+1)/3]^{1/2} \delta_{S,0}$	$\mathcal{J}_{(s,p)}$
$sp(S_1 L_1) dSLJ \rightarrow sp^2 (S_1' L_1') SL'J'$	$(-1)^{L+S+1/2} \sqrt{2} [s_1, s_1', L_1', L]^{1/2}$ $\times \left\{ \begin{array}{ccc} 1/2 & 1/2 & s_1 \\ s & 1/2 & s_1' \end{array} \right\} \left\{ \begin{array}{ccc} 1 & 1 & L_1' \\ 1 & L & 2 \end{array} \right\}$	$\mathcal{J}_{(p,d)}$

TABLE II. Theoretical x-ray energies.

Initial configuration	Initial state	Final configuration	Final state	Energy (eV)
1s2s3s	4S	1s2s2p	4P	139
1s2s3p	$(^1S)^2P$	1s 2 2s	2S	1048
	$(^3S)^2P$		2S	1039
	$(^3S)^4P$		2S	1037
1s2s3p	$(^1S)^2P$	1s2s 2	2S	153
	$(^3S)^2P$		2S	144
	$(^3S)^4P$		2S	142
1s2p3s	$(^1P)^2P$	1s 2 3s	2S	918
	$(^3P)^2P$		2S	912
	$(^3P)^4P$		2S	909
1s2p3s	$(^1P)^2P$	1s2p 2	2S	127
	$(^1P)^2P$		2P	132
	$(^1P)^2P$		2D	134
	$(^3P)^2P$		2S	121
	$(^3P)^2P$		2P	126
	$(^3P)^2P$		2D	128
	$(^3P)^4P$		4P	134
1s2p3p	$(^1P)^2S$	1s 2 2p	2P	1043
	$(^3P)^2S$			1038
	$(^1P)^2P$			1041
	$(^3P)^2P$			1032

TABLE II continued

Initial configuration	Initial state	Final configuration	Final state	Energy (eV)
	$(^1P)^2_D$			1041
	$(^3P)^2_D$			1036
	$(^3P)^4_S$			1032
	$(^3P)^4_P$			1034
	$(^3P)^4_D$			1031
1s2p3p	$(^1P)^2_S$	1s ² 3p	2_P	918
	$(^3P)^2_S$			913
	$(^1P)^2_P$			916
	$(^3P)^2_P$			907
	$(^1P)^2_D$			916
	$(^3P)^2_D$			911
	$(^3P)^4_S$			907
	$(^3P)^4_P$			909
	$(^3P)^4_D$			906
1s2p3p	$(^1P)^2_S$	1s2p2s	$(^1P)^2_P$	154
	$(^3P)^2_S$		$(^3P)^2_P$	141
	$(^1P)^2_P$		$(^1P)^2_P$	152
	$(^3P)^2_P$		$(^3P)^2_P$	135
	$(^1P)^2_D$		$(^1P)^2_P$	151
	$(^3P)^2_D$		$(^3P)^2_P$	139
	$(^3P)^4_S$		$(^3P)^4_P$	155
	$(^3P)^4_P$		$(^3P)^4_P$	157
	$(^3P)^4_D$		$(^3P)^4_P$	154

TABLE II continued

Initial configuration	Initial state	Final configuration	Final state	Energy (eV)
1s2p3d	$(^1P)^2P$	1s ² 3d	2D	920
	$(^3P)^2P$			914
	$(^1P)^2D$			918
	$(^3P)^2D$			910
	$(^1P)^2F$			919
	$(^3P)^2F$			913
	$(^3P)^4P$			912
	$(^3P)^4D$			911
	$(^3P)^4F$			909
1s2p3d	$(^1P)^2P$	1s2p ²	2S	135
			2P	141
			2D	143
	$(^3P)^2P$		2S	129
			2P	135
			2D	136
	$(^1P)^2D$		2S	134
			2P	139
			2D	141
	$(^3P)^2D$		2S	125
			2P	130
			2D	132

TABLE II continued

Initial configuration	Initial state	Final configuration	Final state	Energy (eV)
	$(^1P)^2F$		2S	134
			2P	140
			2D	142
	$(^3P)^2F$		2S	128
			2P	133
			2D	135
	$(^3P)^4P$		4P	143
	$(^3P)^4D$		4P	142
	$(^3P)^4F$		4P	140

TABLE III. Auger and x-ray decay rates (in atomic units^a) and fluorescence yields for states of the $1s2s(S_1L_1)3sSLJ$ configuration of $^{10}_{10}\text{Ne}^{7+}$.

Initial state ^b	Auger rate	X-ray rate ($L_{2,3}$)	Total decay rate	Fluorescence yield $w_{L_{2,3}}$
$(^1S) ^2S_{1/2}$	2.326 (-4)	-	2.326 (-4)	-
$(^3S) ^2S_{1/2}$	6.158 (-4)	-	6.158 (-4)	-
$(^3S) ^4S_{3/2}$	0	1.037 (-6)	1.037 (-6)	1.00

^aOne atomic unit equals $4.134 \times 10^{16} \text{ sec}^{-1} = 27.21 \text{ eV}/\hbar$.

^bState listed is the dominant component in the wavefunction expansion.

TABLE IV. Auger and x-ray decay rates (in atomic units) and fluorescence yields for states of the $1s2s(S_1L_1)3pSLJ$ configuration of $^{10}_{10}\text{Ne}^{7+}$.

Initial state	Auger rate	X-ray rates		Total decay rate	Fluorescence yields	
		K	L_1		ω_K	ω_{L_1}
$(^1S)2P_{1/2}$	4.021(-4)	1.304(-5)	1.055(-6)	41.62(-5)	3.13(-2)	2.53(-3)
$(^3S)2P_{1/2}$	1.723(-4)	3.427(-5)	3.624(-6)	21.02(-5)	0.163	1.72(-2)
$(^3S)4P_{1/2}$	8.941(-8)	1.828(-8)	1.904(-9)	1.096(-7)	0.167	1.73(-2)
$(^1S)2P_{3/2}$	4.025(-4)	1.301(-5)	1.058(-6)	41.66(-5)	3.12(-2)	2.54(-3)
$(^3S)2P_{3/2}$	1.721(-4)	3.427(-5)	3.618(-6)	21.00(-5)	0.163	1.72(-2)
$(^3S)4P_{3/2}$	2.462(-7)	5.038(-8)	5.244(-9)	3.018(-7)	0.167	1.74(-2)

TABLE V. Auger and x-ray decay rates (in atomic units) and fluorescence yields for states of the $1s2p(S_1L_1)3pSLJ$ configuration of $^{10}_{10}\text{Ne}^{7+}$.

Initial state	Auger rate	X-ray rates		Total decay rate	Fluorescence yields	
		K	L_1		ω_K	ω_{L_1}
$(^1P)2S_{1/2}$	5.088(-4)	1.566(-4)	2.618(-6)	66.80(-5)	0.234	0.004
$(^3P)2S_{1/2}$	1.347(-4)	8.519(-5)	2.618(-6)	22.25(-5)	0.383	0.012
$(^1P)2P_{1/2}$	2.318(-6)	2.045(-4)	2.618(-6)	20.94(-5)	0.977	0.013
$(^3P)2P_{1/2}$	7.889(-7)	3.671(-5)	2.618(-6)	4.013(-5)	0.915	0.065
$(^3P)4P_{1/2}$	3.840(-7)	8.144(-7)	2.618(-6)	0.381(-5)	0.214	0.688
$(^3P)4D_{1/2}$	7.390(-9)	3.970(-7)	2.618(-6)	0.302(-5)	0.131	0.868
$(^1P)2P_{3/2}$	1.714(-6)	2.056(-4)	2.618(-6)	20.99(-5)	0.980	0.012
$(^3P)2P_{3/2}$	2.843(-6)	2.892(-5)	2.618(-6)	3.438(-5)	0.841	0.076
$(^1P)2D_{3/2}$	8.169(-4)	1.869(-4)	2.618(-6)	100.64(-5)	0.186	0.003
$(^3P)2D_{3/2}$	6.371(-4)	5.489(-5)	2.618(-6)	69.46(-5)	0.079	0.004
$(^3P)4S_{3/2}$	7.084(-7)	7.380(-6)	2.618(-6)	1.071(-5)	0.689	0.245
$(^3P)4P_{3/2}$	5.530(-7)	1.605(-7)	2.618(-6)	0.333(-5)	0.048	0.787
$(^3P)4D_{3/2}$	9.554(-9)	3.046(-7)	2.618(-6)	0.292(-5)	0.103	0.897
$(^1P)2D_{5/2}$	9.102(-4)	1.791(-4)	2.618(-6)	109.19(-5)	0.164	0.002
$(^3P)2D_{5/2}$	5.459(-4)	6.195(-5)	2.618(-6)	61.05(-5)	0.101	0.004
$(^3P)4P_{5/2}$	3.655(-6)	8.709(-7)	2.618(-6)	0.715(-5)	0.122	0.366
$(^3P)4D_{5/2}$	1.603(-9)	2.334(-7)	2.618(-6)	0.285(-5)	0.081	0.919
$(^3P)4D_{7/2}$	0	0	2.618(-6)	0.262(-5)	0	1.00

TABLE VI. Auger and x-ray decay rates (in atomic units) and fluorescence yields for states of the $1s2p(s_1L_1)3sSLJ$ configuration of $^{10}_{10}\text{Ne}^{7+}$.

Initial state	Auger rate	X-ray rates		Total decay rate	Fluorescence yields	
		K	$L_{2,3}$		ω_K	$\omega_{L_{2,3}}$
$(^1P) ^2P_{1/2}$	1.991(-6)	1.937(-4)	7.639(-7)	19.65(-5)	0.986	0.004
$(^3P) ^2P_{1/2}$	3.915(-4)	2.726(-6)	1.218(-6)	39.55(-5)	0.007	0.003
$(^3P) ^4P_{1/2}$	2.714(-7)	6.562(-8)	6.609(-7)	9.979(-7)	0.066	0.662
$(^1P) ^2P_{3/2}$	6.734(-6)	1.956(-4)	7.943(-7)	20.31(-5)	0.963	0.004
$(^3P) ^3P_{3/2}$	3.864(-4)	6.818(-7)	1.188(-6)	38.83(-5)	0.002	0.003
$(^3P) ^4P_{3/2}$	6.514(-7)	1.978(-7)	6.612(-7)	1.510(-6)	0.131	0.438
$(^3P) ^4P_{5/2}$	0	0	6.607(-7)	6.607(-7)	0	1.00

TABLE VII. Auger and x-ray decay rates (in atomic units) and fluorescence yields for states of the $1s2p(S_1L_1)3dSLJ$ configuration of $^{10}_{10}\text{Ne}^{7+}$.

Initial state	Auger rate	X-ray rates		Total decay rate	Fluorescence yields	
		K	$L_{2,3}$		ω_K	$\omega_{L_{2,3}}$
$(^1P) ^2P_{1/2}$	8.668(-6)	1.840(-4)	7.061(-6)	19.97(-5)	0.921	3.54(-2)
$(^3P) ^2P_{1/2}$	2.932(-7)	1.066(-5)	7.193(-6)	1.814(-5)	0.588	0.396
$(^3P) ^4P_{1/2}$	6.733(-10)	1.805(-8)	6.048(-6)	6.066(-6)	2.98×10^{-3}	0.997
$(^3P) ^4D_{1/2}$	1.507(-8)	3.999(-7)	1.052(-5)	1.094(-5)	3.66(-2)	0.962
$(^1P) ^2P_{3/2}$	8.769(-6)	1.868(-4)	6.975(-6)	20.26(-5)	0.922	3.44(-2)
$(^3P) ^2P_{3/2}$	1.946(-7)	8.006(-6)	7.263(-6)	1.546(-5)	0.518	0.470
$(^1P) ^2D_{3/2}$	3.429(-10)	1.918(-4)	9.558(-6)	20.14(-5)	0.952	4.75(-2)
$(^3P) ^2D_{3/2}$	2.062(-9)	2.947(-6)	4.522(-6)	7.471(-6)	0.394	0.605
$(^3P) ^4P_{3/2}$	1.458(-9)	7.113(-8)	6.409(-6)	6.481(-6)	1.10(-2)	0.989
$(^3P) ^4D_{3/2}$	9.073(-9)	3.078(-7)	1.014(-5)	1.045(-5)	2.95(-2)	0.970
$(^3P) ^4F_{3/2}$	2.107(-11)	3.226(-9)	1.730(-7)	1.762(-7)	1.83(-2)	0.982
$(^1P) ^2F_{5/2}$	2.114(-4)	1.650(-4)	9.085(-6)	38.55(-5)	0.428	2.36(-2)
$(^3P) ^2F_{5/2}$	1.117(-8)	2.964(-5)	5.163(-6)	3.481(-5)	0.851	0.148
$(^1P) ^2D_{5/2}$	2.997(-7)	1.923(-4)	9.498(-6)	20.18(-5)	0.953	4.71(-2)
$(^3P) ^2D_{5/2}$	1.055(-7)	2.289(-6)	4.689(-6)	7.084(-6)	0.323	0.662
$(^3P) ^4P_{5/2}$	4.401(-10)	2.501(-7)	6.955(-6)	7.205(-6)	3.47(-2)	0.965
$(^3P) ^4D_{5/2}$	8.630(-9)	2.753(-7)	9.534(-6)	9.818(-6)	2.80(-2)	0.971
$(^3P) ^4F_{5/2}$	5.440(-8)	2.072(-7)	1.230(-7)	3.846(-7)	0.539	0.320
$(^1P) ^2F_{7/2}$	2.115(-4)	1.585(-4)	9.686(-6)	37.97(-5)	0.417	2.55(-2)
$(^3P) ^2F_{7/2}$	2.537(-7)	3.523(-5)	4.683(-6)	4.016(-5)	0.877	0.117
$(^3P) ^4D_{7/2}$	6.543(-8)	9.557(-7)	1.044(-5)	1.147(-5)	8.33(-2)	0.910
$(^3P) ^4F_{7/2}$	7.003(-8)	3.266(-7)	8.201(-8)	4.786(-7)	0.682	0.171